Behaviour of a Low Frequency Wave in a FRC Plasma

S. Okada, M. Inomoto, T. Masumoto, S. Yoshimura, K. Kitano

Center for Atomic and Molecular Technologies, Osaka University,
Osaka, Japan

e-mail contact of main author: okada@ppl.eng.osaka-u.ac.jp

Abstract. A low frequency torsional wave (angular frequency $\omega \approx (1/3)\omega_{ci0}$, ω_{ci0}; ion gyro frequency in vacuum) is induced in an extremely high beta (beta = plasma pressure / pressure of confining magnetic field) plasma with the field reversed configuration (FRC) by an external antenna which radiates mainly a compressional magnetic perturbation. When the wave propagates from outside toward the magnetic axis of the FRC plasma, not only the Alfven velocity v_A but also the local ion gyro frequency ω_{ci} decreases as the density increases and the magnetic field decreases with decrease of the radial coordinate r. The spatial structure of the wave is examined from around the separatrix to the radial location where the relation $\omega \approx \omega_{ci}$ holds. The amplitude is large at around the separarix $r = r_s$ and it becomes small at the radial location where $\omega \approx (1/2)\omega_{ci0}$, where, the perpendicular wave number $k_\perp$ becomes large. The polarization of the wave is left handed near the separatrix and right handed deep in the plasma. These behaviour is partly explained by the torsional alfven wave with the cold plasma approximation. But, it seems that the kinetic effect is required for the complete understanding of the structure of the wave.

1. Introduction

The FRC plasma[1] has a toroidal geometry even if it is produced in a simple linear solenoidal field. In addition, it has extremely high beta value of 1 at its magnetic axis. These features are desirable for a reactor because higher pressure plasma can be contained in a simple geometry with smaller confining field than in low beta systems. But, different from low beta plasmas, waves with $\omega_{ci} < \omega < \omega_{ce}$ are not accessible[2] to the FRC plasma[3,4] and a low frequency wave is adopted to induce a torsional wave mode converted from a compressional wave launched from an external antenna. In ref.[3,4], in an additional heating experiment of the FRC plasma, two single turn coils displaced axially by 0.6m was used as an antenna. Each coil had the radius of 0.33m and was arranged in such a way as to surround the 0.4m-diameter, 3.4m-long plasma column. Though the wave from the antenna was compressional, as the antenna current flowed in the $r-\theta$ plane (θ is the toroidal direction) at constant r=0.33m and therefore the wave did not have a $\tilde{B}_t$ component, a torsional wave was observed to be induced in the plasma and its dispersion relation was consistent with the Alfven wave in the measurement near and outside the separatrix. Ion heating from 60eV to 80eV was also observed. In ref.[5], the same wave (the torsional wave with the same dispersion relation) was induced even with a small single loop antenna which did not

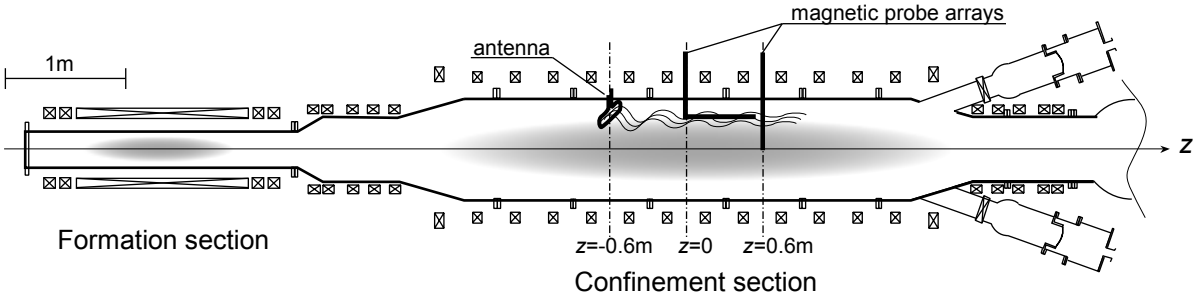

FIG.1 Schematic of the FRC Injection Experiment (FIX) apparatus.

surround the plasma (the anntena current was in the $r-\theta$ plane again). In this case, ion heating was within experimental error partly because the energy supplied to the antenna was 1/4 of the former one. So far, neither the existence of the resonance layer at which the compressional wave is converted to the torsional wave nor the reason for the ion heating was known.

2. Experimental Arrangement

A schematic of our FRC Injection Experiment (FIX) apparatus is shown in Fig.1. The FRC plasma is produced in a 0.31*m*-diameter, 1.6*m*-long formation section of theta pinch of the FIX apparatus, which plasma is injected (translated) into a 0.8*m*-diameter, 3.4*m*-long confinement section[6]. The diameter and the length of the FRC plasma in the confinement section is about 0.4*m* and 3.4*m,* respectively. Typical electron density and the pressure balance temperature are $4\times10^{19}/m^3$ and 80*eV*, respectively. The life time of the configuration is normally about 500μs. But in the present case, it is about 300 μs due to the magnetic probes inserted in the plasma. When the transient phenomena associated with the translation subsided and the plasma is decaying quietly, a magnetic oscillation, the main component of which is the compressional mode, is applied to the plasma by a rectangular-shaped (70*mm* × 250*mm*) one-turn loop antenna. The antenna is arranged at the location displaced by 0.6*m* (z = -0.6*m*) axially from the axial mid-plane (z = 0*m*) of the confinement chamber and by 0.25*m* radially from the axis of the apparatus. It is energized by a capacitor bank and an oscillating magnet field that decays with the e-folding time of about 30μs is radiated. The frequency of the oscillation is about 100*kHz* (ω=600*kc/s*). Behavior of the induced wave is measured by a radial array of magnetic probes arranged at z=0.6*m*, or, displaced by 1.2*m* form the antenna axially. The array consists of 12 sets of magnetic probes each of which records 3 components

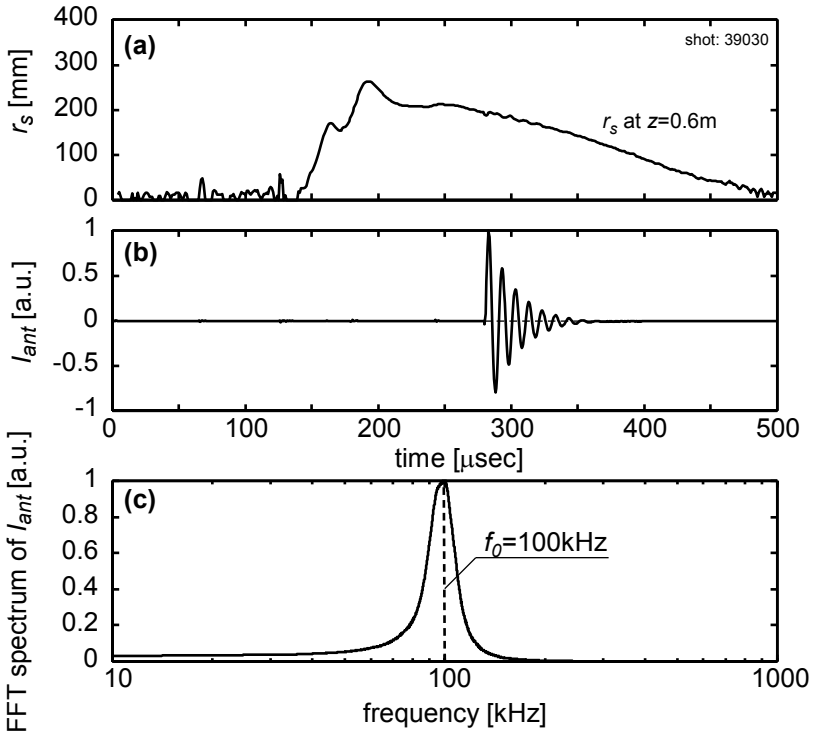

FIG.2 (a) Change of the separatrix radius rs with time at z=0.6m where the probe measurement is carried out. (b) Wave form of the electric current fed to the antenna. (c) Fourier spectrum of the antenna current.

($\tilde{B}_r, \tilde{B}_t, \tilde{B}_z$; t denotes the toroidal or the azimuthal direction and z denotes the axial direction of the magnetic disturbance and is arranged every 20mm radially. They are contained in a 9.4mm diameter boron-nitride sheath in order to minimize the disturbance to the plasma[7]. The magnetic field which is sustaining the configuration is also measured by a similar probe array.

3. Experimental Results

In Fig.2 (a), temporal change of the separatrix radius r_s is shown at z = 0.6m (1.2m from the antenna) where the measurement of the wave is carried out. In Fig.2 (b), wave form of the electric current fed to the antenna, and in Fig.2 (c), its Fourier spectrum are shown. In Fig.3, three components of the magnetic disturbance at z = 0.6m is shown. $\tilde{B}_t$ has a larger amplitude and a higher coherency than other components.

The plasma tends to shift away from the probe and the amount of the shift changes from shot to shot. Profile of the confining magnetic field in Fig.4 (a) is obtained by correcting the shift over 5 shots. The standard deviation is shown as error bars. The origin r = 0 of the horizontal axis refers to the center of the apparatus through which the probe array is set. The reason why the magnetic field reversal is not seen is either the center of the plasma is displaced away from the probe array or the reversal has disappeared at this time. (The reversal is detected by the probe array in the phase of the translation in which the plasma displays not only the axial motion but also the radial and the azimuthal shift motion.) The observation is as such, but, high beta nature is still observed. At r = 0, the beta value is 71% and the magnetic field is 54% of the external field strength. As the confining magnetic field decreases from outside toward inside the plasma, the value of the local ion gyro frequency ω_{ci} decreases accordingly. At r = 300mm, ω=0.36 ω_{ci} and at r = 0, ω=0.67ω_{ci}. In Fig.4 (b), spatial profiles of $\tilde{B}_t$ amplitude for 5 shots and their temporal development are displayed. The amplitude is large at

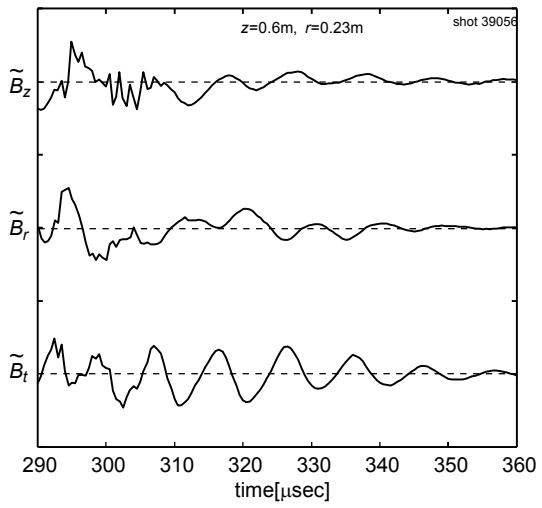

FIG.3 Three components of the magnetic disturbance at z=0.6m. $\tilde{B}_t$ has larger amplitude and higher coherency than other components

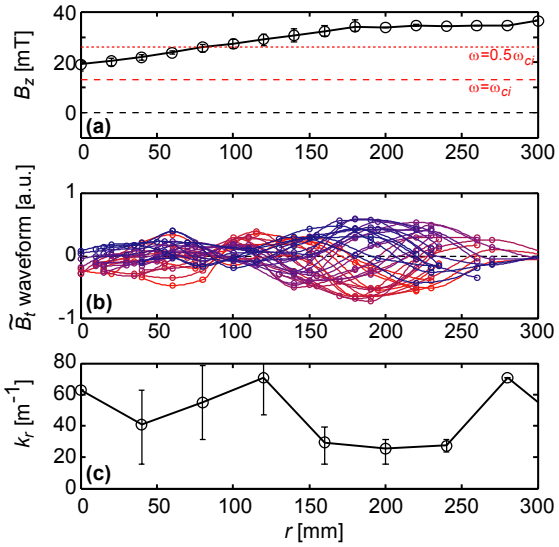

Fig.4 (a) Ratdial profile of the confining magnetic field. (b) Radial structure and temporal behavior of $\tilde{B}_t$ (5 shots). The amplitude is large at around r=200mm and is small at around r=100mm. (c) Radial structure of the radial (perpendicular) wave number k_r.

around $r = 200mm$ and is small at around $r = 100mm$. Finite amplitude is observed over all the radial location. Perpendicular phase velocity v_p of $\tilde{B}_t$ is calculated from the data of the probe array, and the radial wave number k_r is obtained by ω / v_p. In Fig.4 (c) k_r is plotted. It becomes large at around $r = 100mm$. In Fig.5, polarization of $\tilde{B}$ at various location is shown together with the amplitude of $\tilde{B}_t$. The polarization is left handed near and outside the separatrix and is right handed deep inside the plasma. Between these two regions, the polarization is nearly linear.

4. Discussion

Behavior of the tortional Alfven wave is examined by a theory based on a cold plasma approximation with the Hall term included [8]. The torsional Alfven wave has a resonance at a radial location where $k_\perp^2 = \infty$ (denoted as $k_r^2 = \infty$ in the case of experiment) is satisfied, where, $k_\perp^2 = (F^2 - G^2)/F$, $F = A - k_{//}^2$, $G = (\omega/\omega_{ci})A$, $A = \omega^2/(v_A^2(1-(\omega/\omega_{ci})^2))$. Therefore, the resonance point is obtained from $k_{//}^2 = \omega^2/(v_A^2(1-(\omega/\omega_{ci})^2))$ using measured $k_{//}$, the magnetic field profile and the density profile. If we assume that the temperature is uniform, the density profile is calculated from the measured magnetic field profile via the pressure balance equation. Using this equation, at the resonance point $n/n_0 = (1-A_G)/(1+A_G)$ or, $B/B_0 = (A_A + A_G)/(1+A_G)$ where, $A_A = \omega^2/(k_{//}v_{A0})^2$ and $A_G = (\omega/\omega_{ci0})^2$. With measured $k_{//} = 3.3/m$, $n/n_0 = 10-20\%$ and therefore, $B/B_0 \approx 90\%$, the resonant point is obtained to be $r = r_{reso} \approx 150mm$. As $F = k_{//}^2(A/k_{//}^2 - 1)$

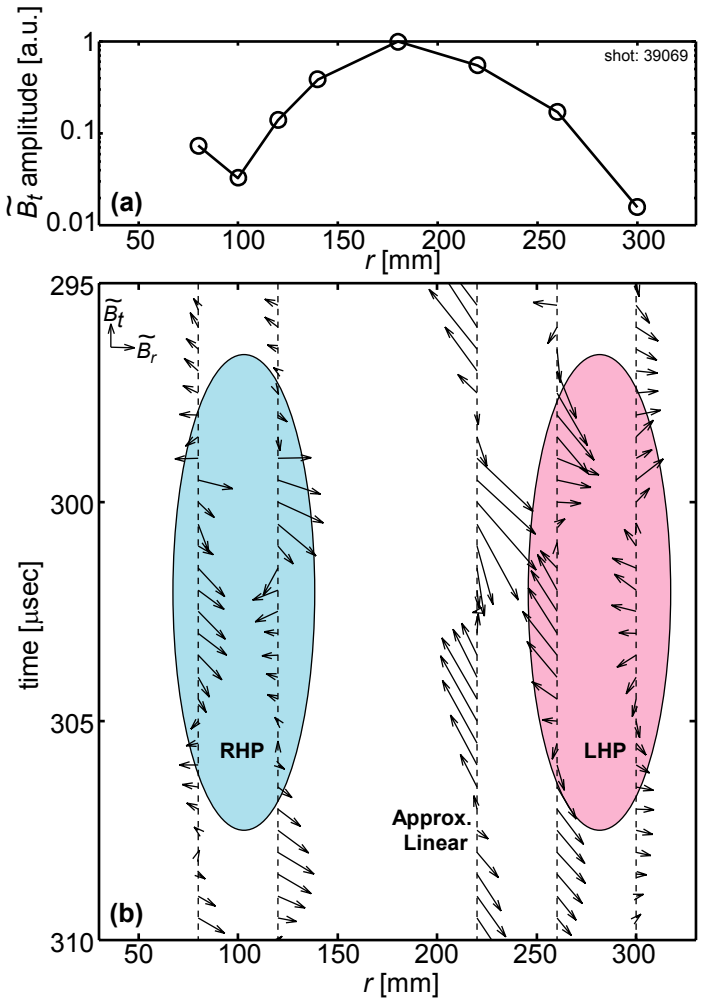

Fig.5 (a) Amplitude and (b) Spatial structure of the magnetic disturbance.

and $F^2 - G^2 = ((1 - k_{//}^2 / A)^2 - (\omega / \omega_{ci})^2) A^2$, considering the fact that $k_{//}^2 / A = (v_A^2 / (\omega / k_{//})^2)(1 - (\omega / \omega_{ci})^2)$, for $r >> r_{reso}$, $F < 0$, and $F^2 - G^2 > 0$, because the plasma is tenuous and v_A is large, and therefore, $k_\perp^2 < 0$. On the other hand, just outside $r = r_{reso}$, $F > 0$ and $F \approx 0$. Therefore, $F^2 - G^2 < 0$ and $k_\perp^2 > 0$ and further, $k_\perp^2$ becomes large when r approaches r_{reso}. Different from the theory, k_r ($k_\perp$ in the theory) does not become large in the experiment near the resonant point. The observation that $\tilde{B}_t$ becomes small at $r \approx 100mm$ where, $\omega \approx 0.5\omega_{ci}$, can not be explained by the theory either. Here, the sound velocity c_s is larger than v_A and the kinetic effect which is neglected in the cold plasma theory may be important[2,8,9,10].

The torsional Alfven wave propagates predominantly in z direction, the polarization of the magnetic disturbance is given by $\tilde{B}_t / i\tilde{B}_r = (A\omega / \omega_{ci}) / F$. In Fig.6, spatial dependences of $k_\perp^2$ and $\tilde{B}_t / i\tilde{B}_r$ are shown together with the magnetic field profile. The polarization is right handed deep in the plasma and outside, vice versa. This is consistent with the experimental observation (Fig.5) qualitatively. The position of the resonance point is $r \approx 150mm$ in the theory, and $r \approx 220mm$ in the experiment. The difference is not significant. Because the magnetic field profile is flat around this radial location and small difference in magnetic field strength causes large difference in r.

5. Summary

Behavior of the low frequency torsional Alfven wave which enabled ion heating of the FRC plasma with extremely high beta value, in which not only the density but also the magnetic field had strong spatial variation. Spatial structure of the polarization of the magnetic perturbation (right handed deep in the plasma and left handed outside) could be explained by

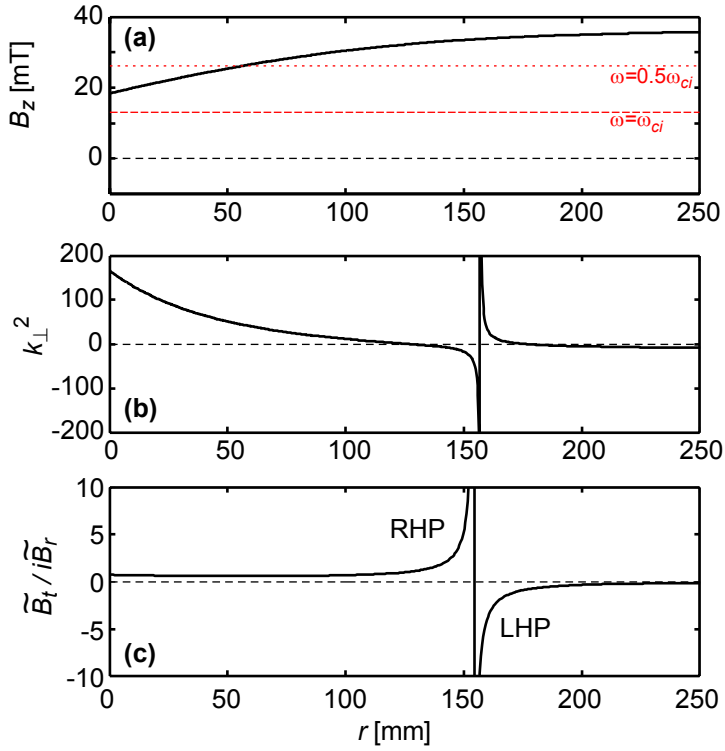

Fig.6 Spatial dependences of (b) and (c) obtained by the cold plasma approximation for the magnetic field profile given in (a). The polarization is right handed deep in the plasma and outside, vice versa.

the cold plasma approximation. On the other hand, spatial structure of the amplitude of the wave and $k_\perp$ deep in the plasma where $c_s > v_A$ holds could not be explained.

References

[1] Tuszewski, M., “Field reversed configurations”, Nuclear Fusion **28** (1988) 2033
[2] Stix, T. H., Waves in Plasmas, American Institute of Physics, New York, 1992
[3] Yamanaka, K., et al., “Heating experiment of field reversed configuration plasma by low-frequency magnetic pulse”, Phys. Plasmas **7** (2000) 2755
[4] Okada, S., et al., “Experiments an additional heating of FRC plasmas”, Nuclear Fusion **41** (2001) 625
[5] Okada, S., et al., “Excitation and propagation of low frequency wave in a FRC plasma” ,Nuclear Fusion **43** (2003) 1140
[6] Himura, H., “Rethermalization of a field-reversed cponfiguration plasma in translation experiments, Phys. Plasmas **2** (1995) 191
[7] Slough, J. T., Miller, K. E., "Small, high frequency probe for internal magnetic field measurements in high temperature plasmas", Rev. Sci. Instrum, 72(2001) 417
[8] Rodney Cross, An Introduction to Alfven Waves, Adam Hilger, Bristoland Philadelphia, IOP Publishing Ltd 1988
[9] Iwasawa, N., et al. “Global eigenmodes of low frequency waves in field-reversed configuration plasmas”, Phys. Plasmas **11** (2004) 615
[10] Hasegawa, A., Chen, L., “Kinetic processes in plasma heating by resonant mode conversion of Alfven wave”, Phys. of Fluids **19** (1976) 1924